Supporting Information for

Altering peroxymonosulfate activation path for $^1O_2$ production on ZIF-67 with coordinatively unsaturated metal sites

Hongyan Liu[a], Wanting Hui[a], Heyu Gao[a], Guangjie Qu[c], Wenwen Lv[a], Xu Guo[a], Zixin Li[a], Bingbing Li[a], Maoquan Wu[b], Tongjie Yao[b,*], Jie Wu[a, *]

[a]*Key Laboratory of Functional Inorganic Material Chemistry, Ministry of Education, School of Chemistry and Materials Science, Heilongjiang University, Harbin, China*

[b]*School of Chemistry and Chemical Engineering, Harbin Institute of Technology, Harbin, China*

[c]*Jilin Chemical Fertilizer Factory*

*Corresponding authors.

E-mail address: wujie@hlju.edu.cn (J. Wu); yaotj@hit.edu.cn (T. Yao)

Text S1. Materials

$Co(NO_3)_2·6H_2O$, NaOH, HCl, NaN_3, NaCl, $NaNO_3$, Na_2SO_4, $NaHCO_3$, NaH_2PO_4, Na_2CO_3, $K_2Cr_2O_7$, KI, PMS, 2-MeIM, diethylamine, ethanol, VAN, methanol (MeOH), tetraethyl orthosilicat (TEOS), furfuryl alcohol (FFA), *tert*-butylalcohol (TBA), humic acid (HA), methyl blue (MB), rhodamine B (RhB), metronidazole (MTZ), tetracycline (TC), chlortetracycline (CTC), 2,2,6,6-tetramethylpiperidine-1-oxyl (TEMPO), 2,2,6,6-tetramethyl-4-piperidino (TEMP) and 5,5-Dimethyl-1-pyrroline N-oxide (DMPO) were purchased from China Pharmaceutical Chemical Reagent Co. Ltd. All chemicals were analytical grade and used as received. The deionized water was purified through a Millipore system with a resistivity of 18.2 $M\Omega·cm^{-1}$.

Text S2. Calculation method of k value.

To determine k value, the degradation curve of VAN-ZIF-1@Co_2SiO_4 was fitted and calculated. Eq. S1 and S2 were used to express the pseudo-first-order kinetic equation and pseudo-second-order kinetic equation, respectively, where C_0 was the initial MB concentration and C was the MB concentration at time t. According to the higher R^2 values, pseudo-second-order kinetic equation was preferred in this work.

$$k = \frac{-\ln[C / C_0]}{t} \tag{S1}$$

$$\frac{1}{C} - \frac{1}{C_0} = kt \tag{S2}$$

Text S3. Homogeneous Fenton-like reaction

After heterogeneous Fenton-like reaction, the catalysts were removed from solution *via* filter membrane with the pore size of 0.45 μm. The filtrate was heated to 90 ℃ for 2.0 h, and then naturally cooled to room temperature. 24.0 h later, the residual PMS and ROSs are exhausted. 1.0 mL of MB solution (1.0 mg/mL) was added into the filtrate, and then the solution volume was adjusted to 50 mL by water.

Finally, 6.0 mg of PMS was re-added under stirring to start the homogeneous Fenton-like reaction.

Text S4. Evaluation of PMS utilization efficiency

Firstly, KI solution was prepared by dissolving KI (166 mg) and $NaHCO_3$ (40 mg) into 100 mL of water. PMS (6.0 mg) was added into 50 mL of aqueous solution containing 1.25 mg of MB and 2.0 mg of various catalysts. Then, 0.1 mL of supernatant were sampled every 2.0 min, and then injected into 4.9 mL of KI solution. After reaction for 5.0 min, PMS concentration was measured on the Labtech UV-1780 spectrometer based on the absorption peak at 352 nm.

Fig. S1. SEM images and the corresponding length size distributions of (a_1, a_2) ZIF-67; (b_1, b_2) VAN-ZIF-0.2; (c_1, c_2) VAN-ZIF-1; (d_1, d_2) VAN-ZIF-2.

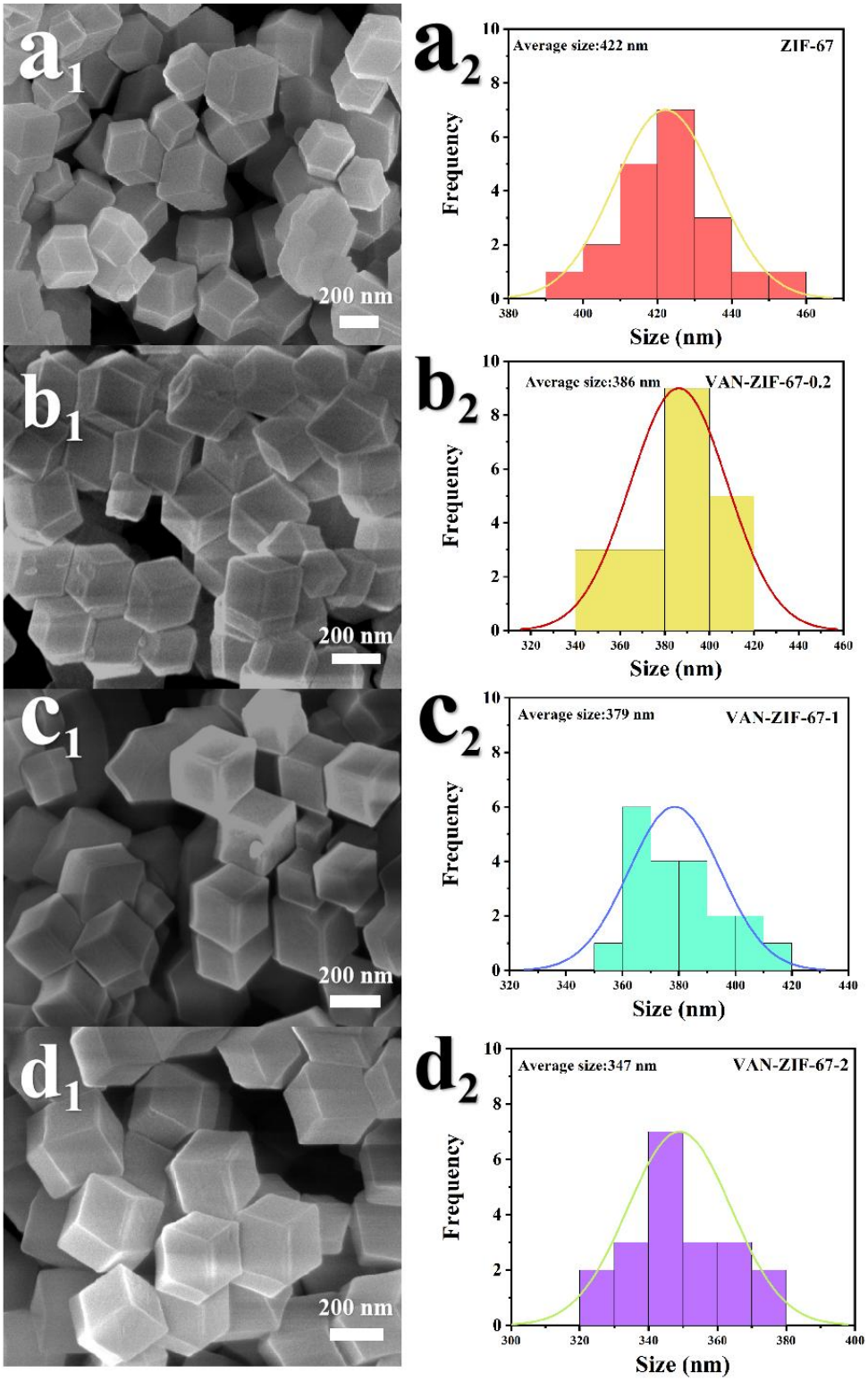

Fig. S2. TEM images and the corresponding length size distributions of (a_1, a_2) ZIF-67@Co_2SiO_4; (b_1, b_2) VAN-ZIF-0.2@Co_2SiO_4; (c_1, c_2) VAN-ZIF-1@Co_2SiO_4; (d_1, d_2) VAN-ZIF-2@Co_2SiO_4.

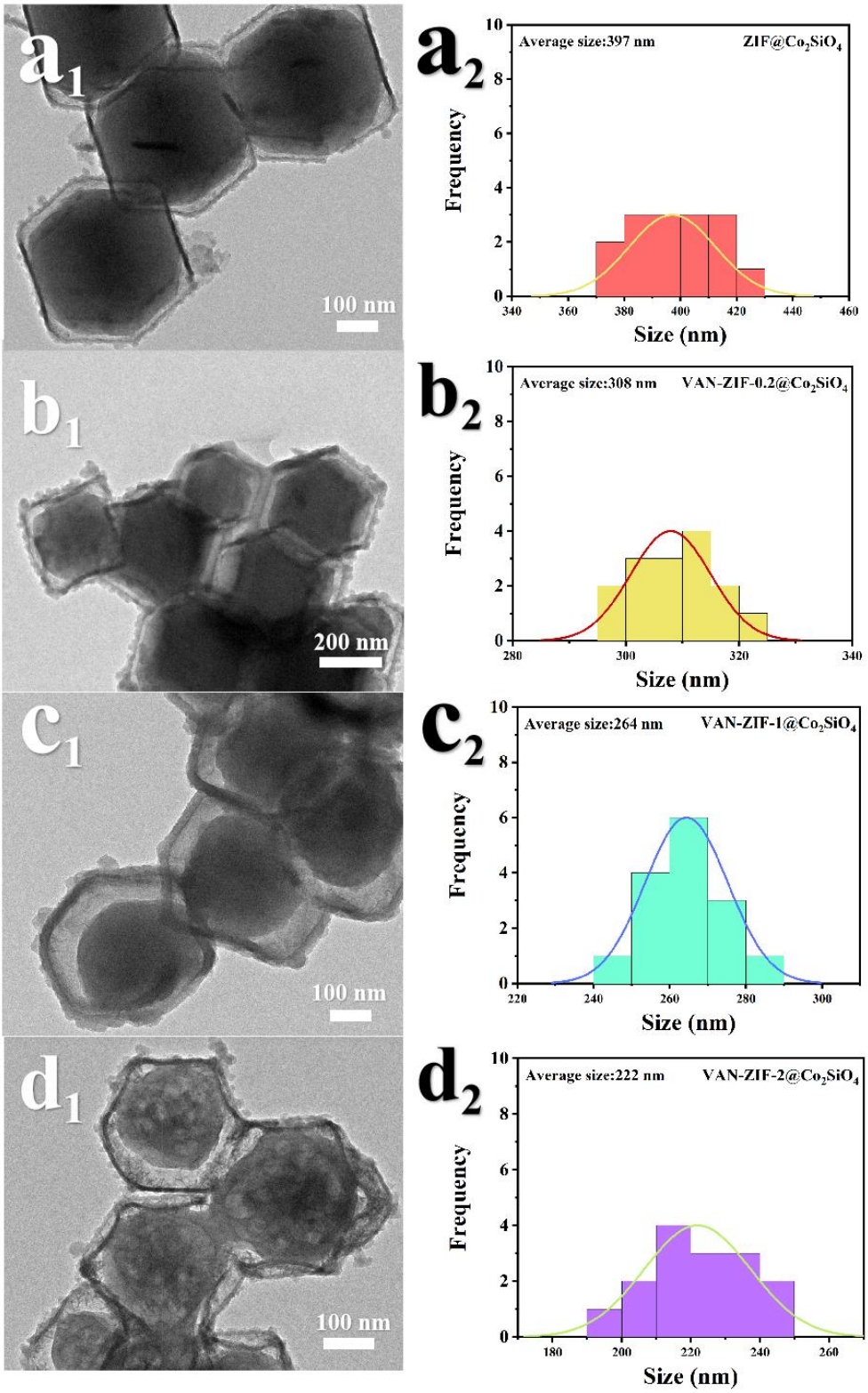

Fig. S3. (a) N_2 adsorption-desorption isotherms and (b) pore size distribution of VAN-ZIF-1@Co_2SiO_4.

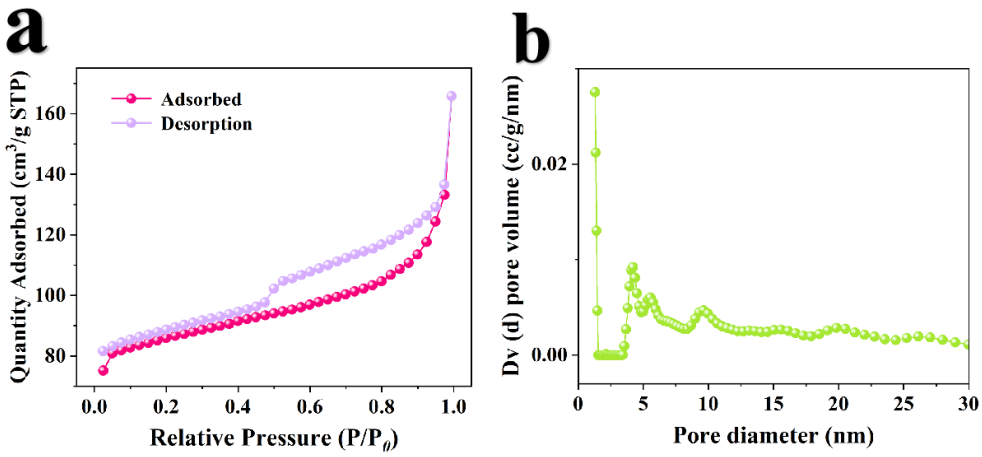

Fig. S4. EDS analysis of (a) VAN-ZIF-1@Co_2SiO_4 and (b) ZIF@Co_2SiO_4.

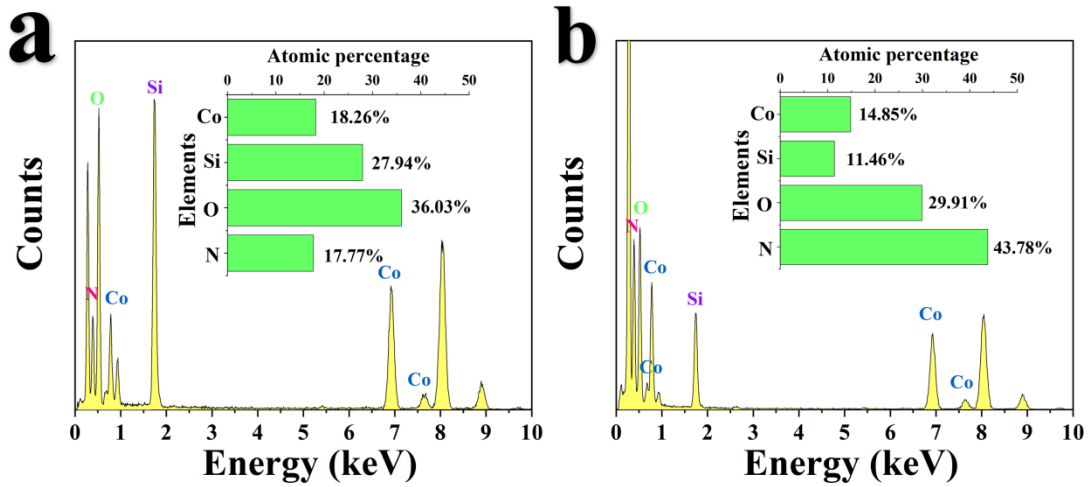

Fig. S5. EDS line scan analysis of VAN-ZIF-1@Co_2SiO_4.

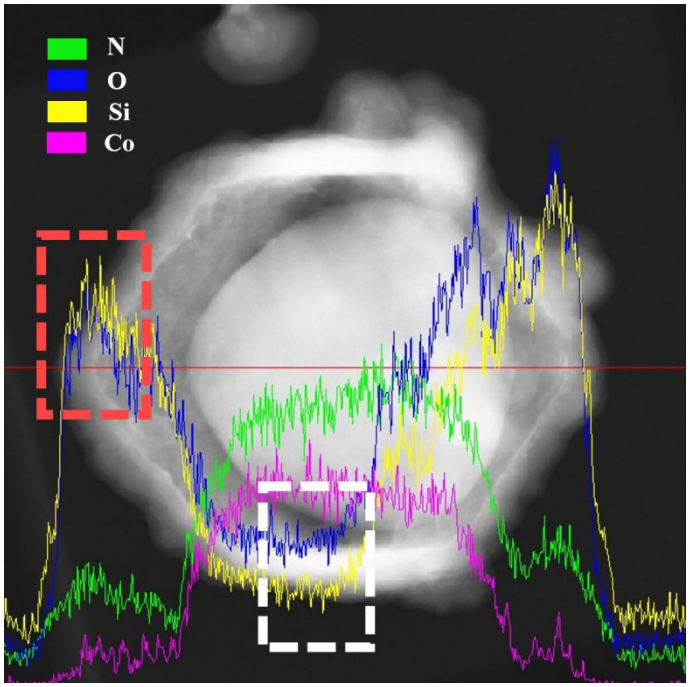

Fig. S6. UV-Vis spectra of $Co(NO_3)_2$, 2-MeIM and as-prepared ZIF-67.

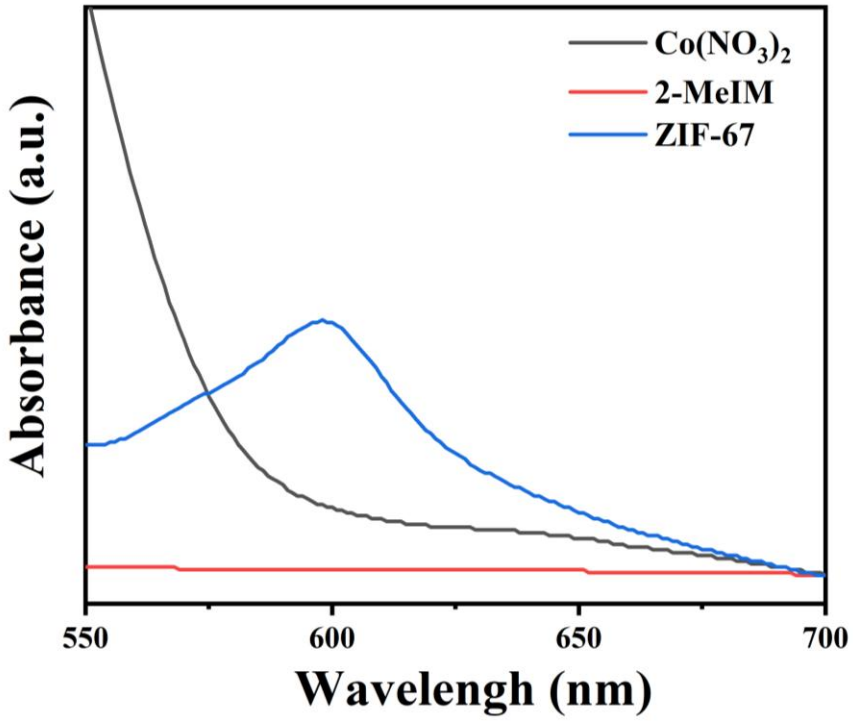

Fig. S7. XRD patterns of ZIF@Co_2SiO_4 and VAN-ZIF-1@Co_2SiO_4.

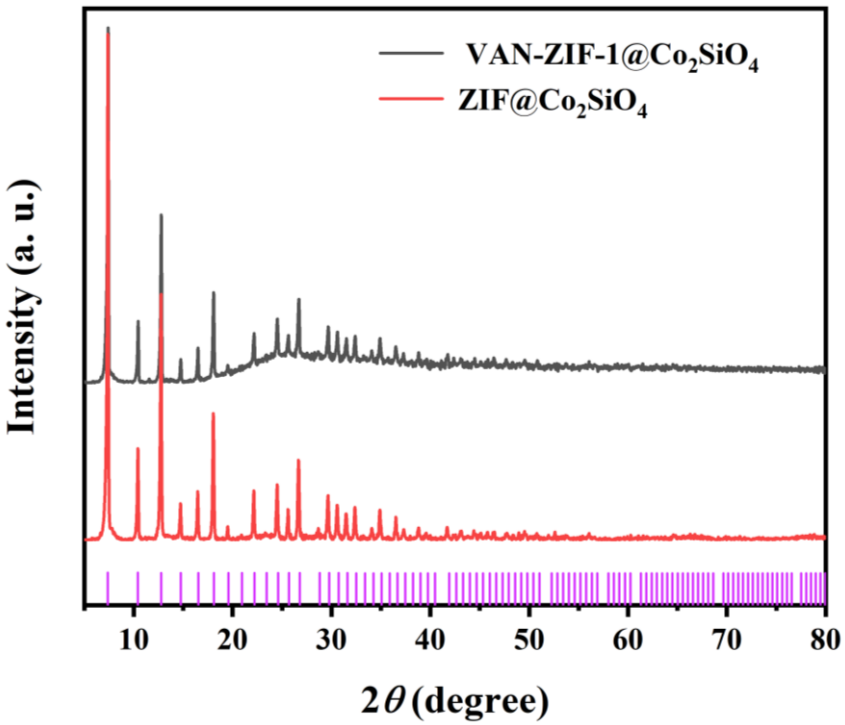

Fig. S8. MB adsorption profiles in the presence of VAN-ZIF-1@Co_2SiO_4. Negative times represented the adsorption process.

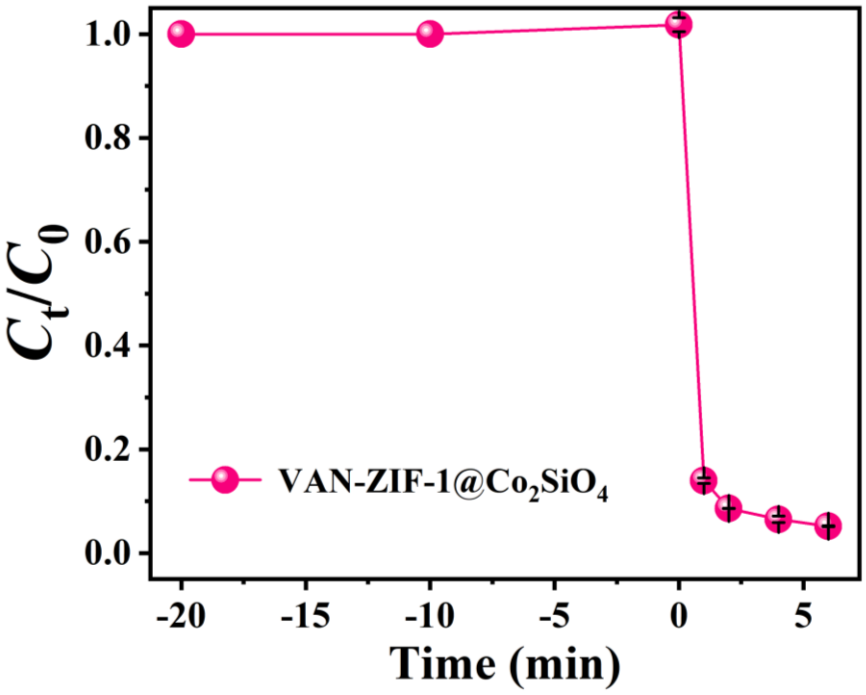

Fig. S9. Parameters on MB degradation process in the presence of VAN-ZIF-1@Co_2SiO_4: (a) PMS dosages. (b) Catalyst dosages. (c) MB concentrations. (d) Solution pH values.

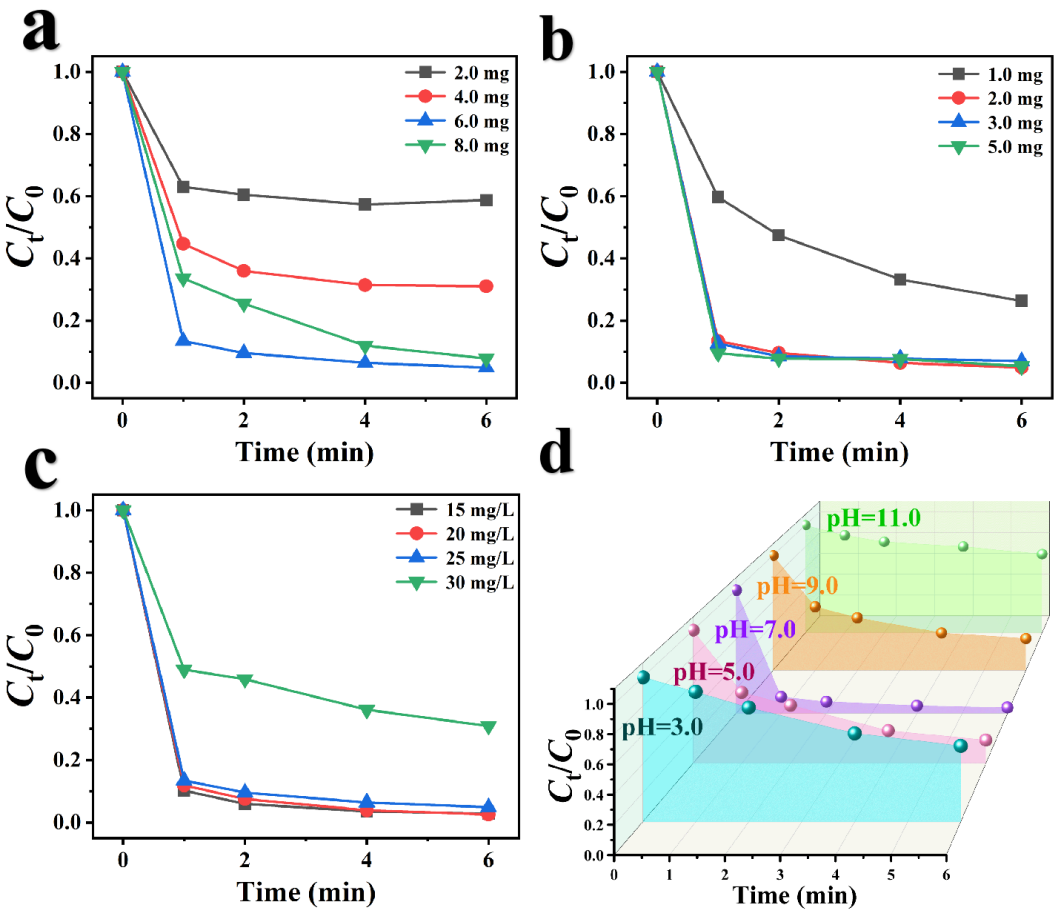

Fig. S9a shows the influence of PMS dosages on MB degradation. When PMS dosages increase from 2.0 to 6.0 mg, the degradation efficiency at 6.0 min sharply increases from 41.2% to 95.1%, owing to the more ROSs yield. Further increasing to 8.0 mg, the degradation efficiency decreases from 93.4% to 92.2%, due to the self-quenching reaction caused by overused PMS. Therefore, 6.0 mg is the optimized PMS dosage.

In Fig. S9b, when catalyst amount increases from 1.0 to 2.0 mg, the degradation efficiency increases from 73.7% to 95.1%, due to the more active sites on catalyst surface. Further increasing to 3.0 and 5.0 mg, the degradation efficiency does not significantly increase. Therefore, 2.0 mg is the optimized catalyst dosage.

The influence of MB concentrations on the degradation efficiency is shown in

Fig. S9c. The degradation efficiency monotonously decreases with the increase of MB concentrations from 15 to 30 mg/L. Herein, 25 mg/L of MB solution is selected as the optimized concentration.

Fig. S9d shows the MB degradation process over VAN-ZIF-1@Co_2SiO_4 under different solution pH values. The maximum degradation efficiency is realized at pH = 7.0, and this is closely related to the catalyst surface charges (see Fig. S10). At 6.0 min, the degradation efficiency under pH = 3.0, 5.0, 9.0 and 11.0 is 47.4%, 82.4%, 72.2% and 26.8%, respectively. This indicates the catalysts show the outstanding activity under weakly acidic, neutral, and weakly alkaline conditions. Under the strong alkaline condition (pH=11.0), HSO_5^- was hydrolyzed to SO_5^{2-} and $Co(OH)_2$ formed on ZIF-67 surface, which reduced the catalytic activity. Under strongly acidic condition (pH=3.0), the degradation efficiency is remarkably reduced, since the $SO_4^{\bullet-}$ is quenched by excess H^+.

Fig. S10. Zeta potentials of VAN-ZIF-1@Co_2SiO_4 in solutions with different pH values.

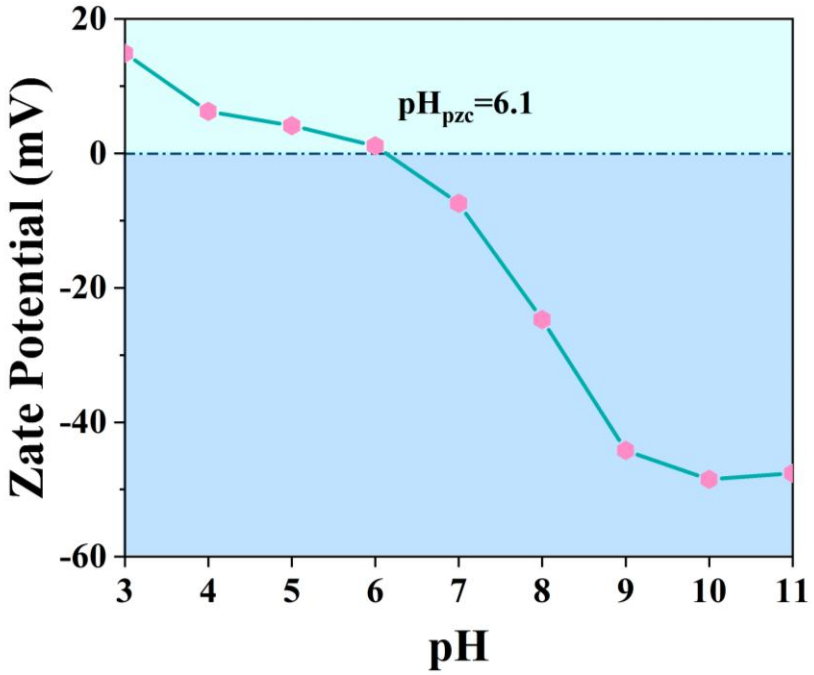

When 3.0 ≤pH≤ 5.0, the catalyst surface was positively charged. Meanwhile, MB mainly existed in the form of MB^+ (Applied Catalysis B: Environmental, 2023, 338, 123059). Therefore, the adsorption of MB on catalyst surface was poor due to the electrostatic repulsion, leading to the inferior degradation performance (Fig. S9d).

The pH_{pzc} of VAN-ZIF-1@Co_2SiO_4 was 6.1 (Fig. S10). Under solution pH=7.0, the catalyst was slightly negatively charged, while MB molecules mainly existed in the form of MB^0, the electrostatic repulsion between catalyst surface and MB molecules was disappeared. Therefore, the maximum degradation efficiency was achieved when 5.0 <pH< 9.0 (Fig. S9d).

When pH> 9.0, MB molecules mainly existed in form of MB^- (Journal of Hazardous Materials, 2022, 436, 129234). The electrostatic repulsion was primary between catalyst surface and MB dyes. In this case, the degradation efficiency was reduced.

Fig. S11. MB degradation profiles in presence of VAN-ZIF-1@Co_2SiO_4 and ZIF-67.

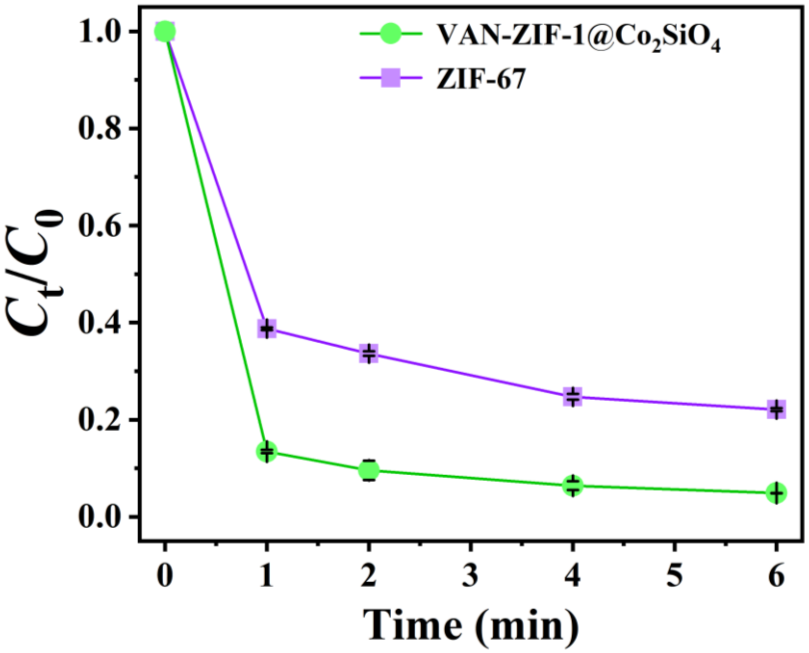

Fig. S12. *k* values calculated by (a) pseudo-first-order kinetic equation, and (b) pseudo-second-order kinetic equation over VAN-ZIF-1@Co_2SiO_4 in Fenton-like reaction. (c) *k* values estimated according to pseudo-second-order kinetic equation of various catalysts in Fenton-like reaction.

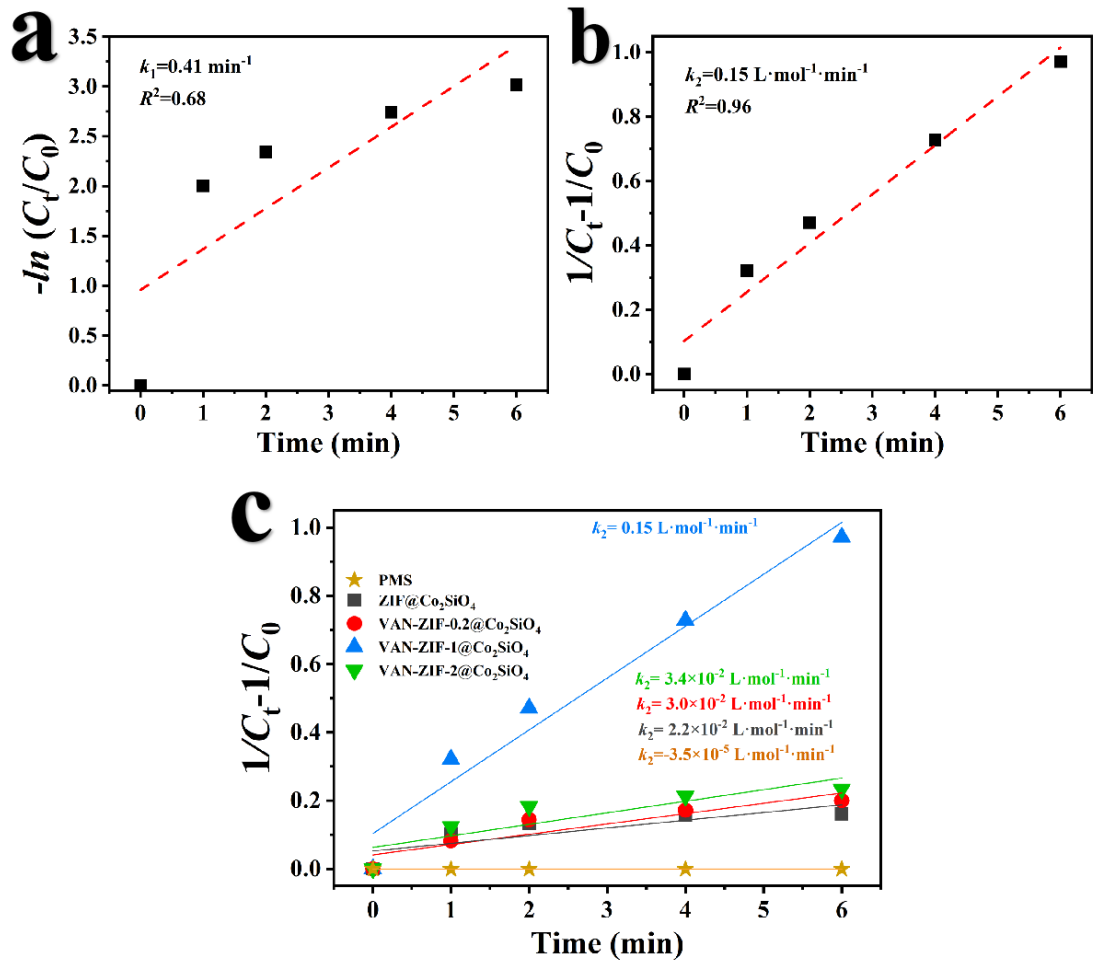

Fig. S13. (a) MB degradation profiles in presence of VAN-ZIF-1@Co_2SiO_4 and ZIF@Co_2SiO_4. (b) Homogeneous Fenton-like reaction triggered by the leached metal ions from VAN-ZIF-1@Co_2SiO_4 and ZIF@Co_2SiO_4.

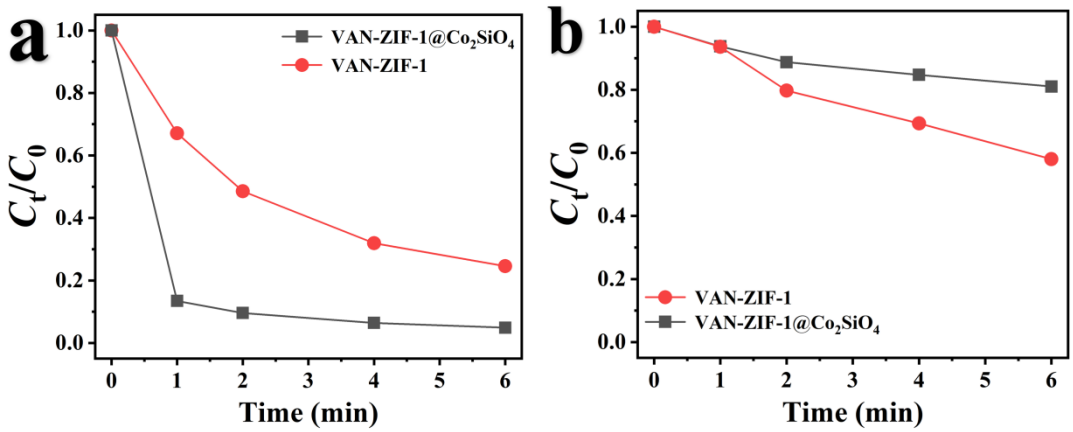

Fig. S14. MB degradation processes in real environmental condition: water from *Songhua River* and Tap water.

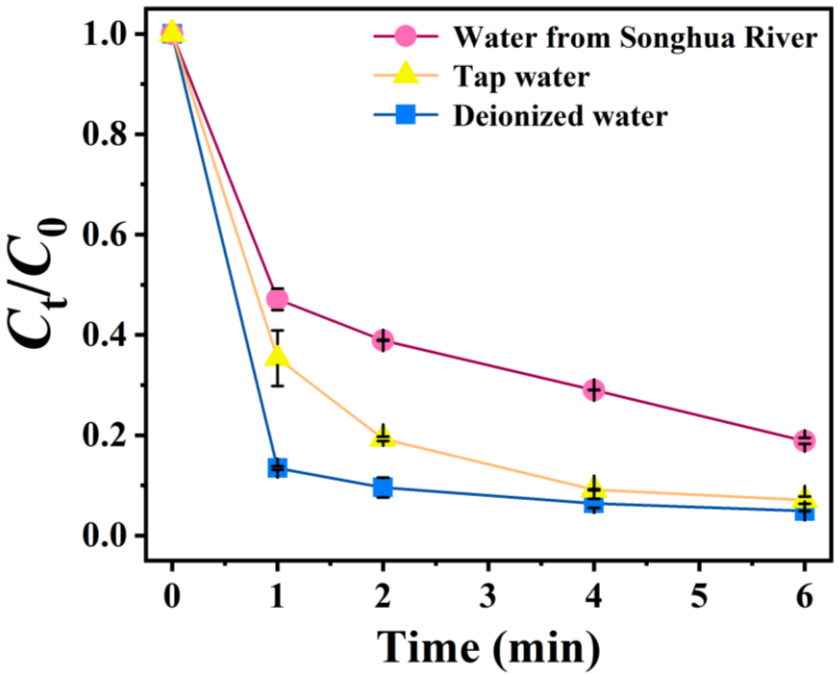

Fig. S15. XRD patterns of fresh VAN-ZIF-1@Co_2SiO_4 and samples after the 4th cycle.

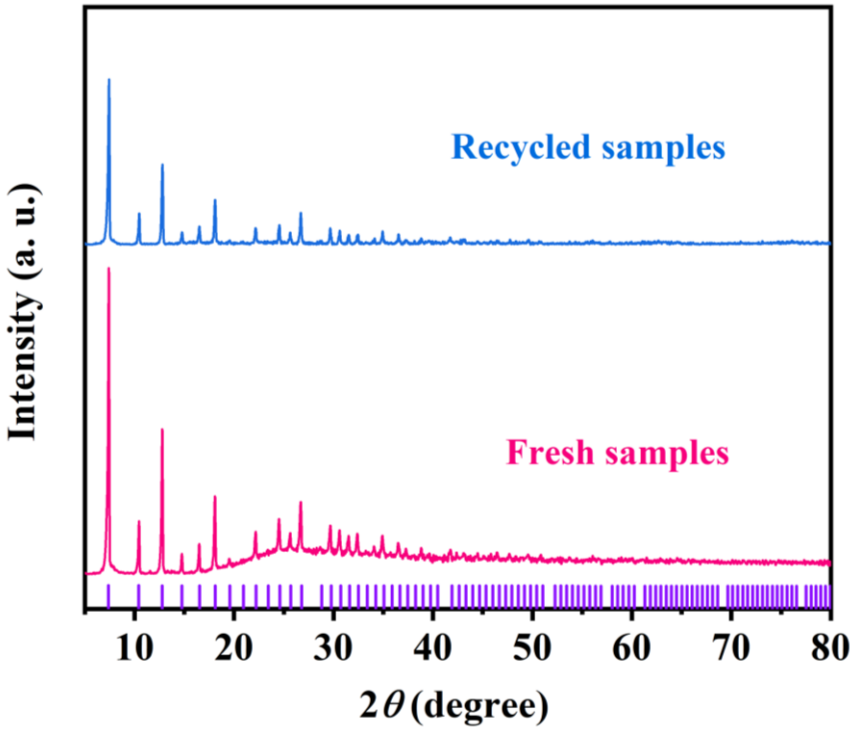

Fig. S16. SEM images of VAN-ZIF-1@Co_2SiO_4 before and after the 4^{th} cycle.

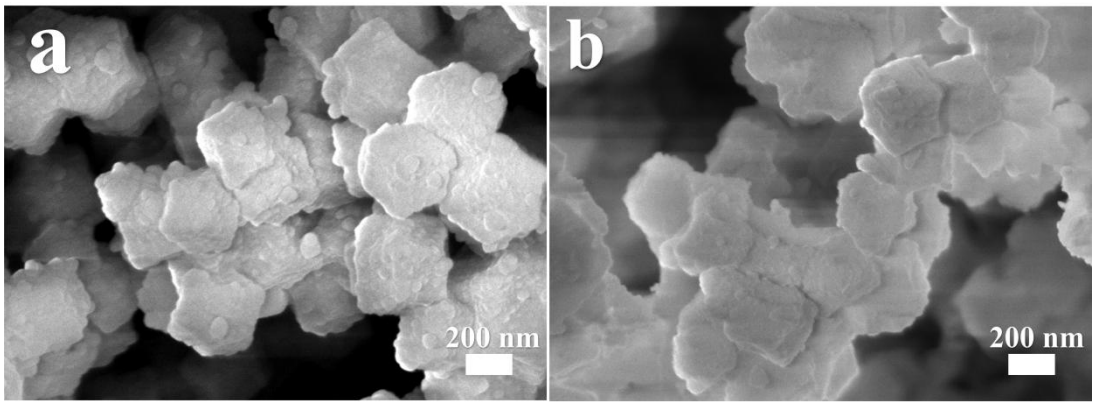

Fig. S17. Scavenger trapping experiment in the system of VAN-ZIF-1@Co_2SiO_4+PMS under the different scavenger dosages.

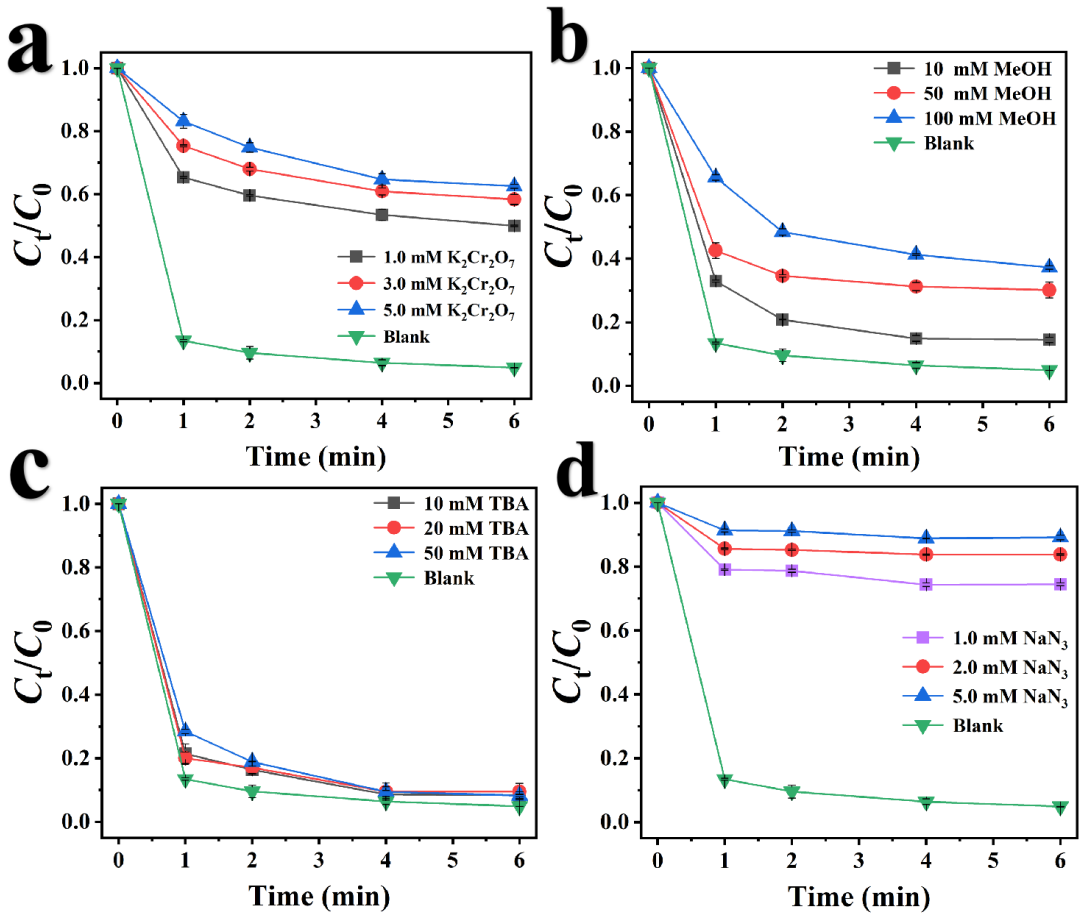

Fig. S18. MB degradation process in D_2O aqueous solution (1/22, v/v).

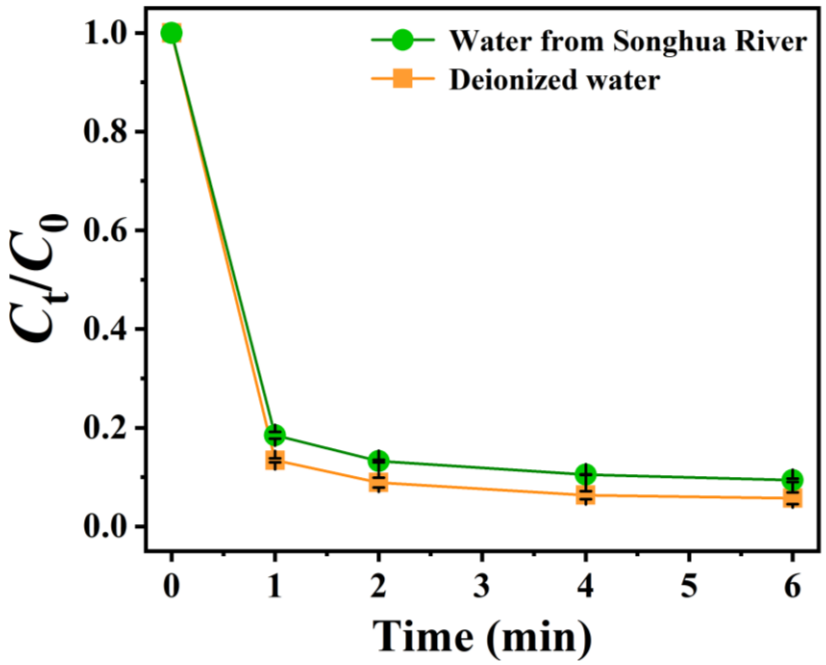

Fig. S19. Radical trapping experiment for MB degradation in Fenton-like reaction with various scavengers over (a) ZIF@Co_2SiO_4; (b) repaired-VAN-ZIF-1@Co_2SiO_4.